Chemical Science

ROYAL SOCIETY OF CHEMISTRY

EDGE ARTICLE

View Article Online
View Journal | View Issue

Cite this: *Chem. Sci.*, 2023, **14**, 8592

All publication charges for this article have been paid for by the Royal Society of Chemistry

Received 6th May 2023
Accepted 17th July 2023

DOI: 10.1039/d3sc02313c

rsc.li/chemical-science

Nitrogen Trifluoride Complexes of Group 10 Transition Metals M(NF_3) (M = Pd, Pt)†

Guohai Deng,* Yan Lu, Tony Stüker and Sebastian Riedel *

The group 10 transition metal atoms Pd and Pt react with nitrogen trifluoride (NF_3) forming N-coordination M(NF_3) complexes in solid neon and argon matrices. The M(NF_3) complexes isomerize to more stable fluoronitrenoid $FNMF_2$ isomers *via* fluorine migration upon blue LED (λ = 470 nm) light irradiation. These products are characterized on the basis of infrared absorption spectroscopy with isotopic substitutions and theoretical frequency calculations. The analysis of the electronic structure of nitrogen trifluoride complexes indicates that the bonding between metal and nitrogen trifluoride can be described as σ donation from the HOMO of nitrogen trifluoride to the empty metal d_{z^2} orbital and π back-donation from the metal $d_{xz/yz}$ orbitals to the LUMO of nitrogen trifluoride, the latter of which stabilized the metal ligand bond and destabilized the ligand N–F bond. In $FNMF_2$, the FN ligand doubly bonded to the metal and bear imido character.

Introduction

Metal–ligand bonding is crucial to transition metal chemistry. The nature and strength of bonding between the metal and ligand determine the stability, geometry and reactivity of intermediates in catalytic reactions.[1] Thus, understanding the nature of the metal–ligand bond is very important.[2,3] Nitrogen trifluoride (NF_3) is a stable and long known compound and was first synthesized by Otto Ruff and co-workers *via* the electrolysis of a HF/NH_4F mixture in 1928.[4] Although it has been widely used as a reactant in gas-phase reactions[5] and synthetic chemistry,[6] the coordination chemistry of this molecule as a Lewis base has received less attention, which is most likely due to its weak Lewis base character. Nevertheless, the proton affinity of NF_3 has been experimentally measured many times since 1980.[7] Experimental and theoretical investigation on the complexes of NF_3 with Lewis acids, such as $BH_{3-n}F_n$ (n = 0–3)[8] and AlH_3 (ref. 9), indicated that nitrogen trifluoride can act as a nitrogen donor to form H_3B–NF_3, F_3B–NF_3 and H_3Al–NF_3 adducts. Nitrogen trifluoride complexes of coinage metals Cu, Ag and Au supported by ligands such as cyanogen and halides were studied by density functional theory.[10] In addition, theoretical studies on the metal ligand back-bonding in Pd(NF_3) and LPd(NF_3) (L = NH_3, PH_3, CO) complexes using NBO analysis demonstrated that the NF_3 ligand also has a strong π acceptor character.[11] Besides the neutral complexes, some nitrogen trifluoride ion complexes have also been studied computationally.[12] It was found that the H^+, Li^+, Na^+ and K^+ nitrogen trifluoride complexes appear to form ion–dipole interactions and the Li^+, Mg^+ and Be^+–NF_3 cations could be detected as stable products in the gas phase.

Recently, reactions of group 4, 6, 8, 9, and 11 metals, Th, and U with nitrogen trifluoride in excess neon and argon have been studied, and difluoroamino, fluoronitrenoid and nitride metal complexes (F_2NMF, $FNMF_2$, and NMF_3) have been prepared and characterized by matrix-infrared spectroscopy and theoretical calculations.[13–16] In contrast to the nitrogen trifluoride reactions reported above, the analogue ammonia molecule reacted with metal atoms to form M(NH_3) complexes first, which rearranged to $HMNH_2$ *via* N–H bond insertion upon light excitation.[17] The weak N–F bond, which is only about half as strong as the N–H bond in the NH_3 molecule,[18] makes the insertion reaction easier than that for the N–H bond. This may result in the spontaneous formation of N–F bond insertion complexes. Moreover, fluorine is the most electronegative element, the lone pair electronic density in the nitrogen atom of NF_3 is decreased, and the dipole moment direction is also reversed as compared with those of NH_3,[19] both of which make it less favourable to give the M(NF_3) complex with a M–N interaction. To the best of our knowledge, there are no experimental reports on the nitrogen trifluoride metal coordination in which the NF_3 ligand does not immediately react further. Here we report the preparation of the nitrogen trifluoride complexes of group 10 metals M(NF_3) (M = Pd, Pt) from laser ablated metal atoms with NF_3 molecules and their spectroscopic identification in low-temperature neon and argon matrices. The nitrogen-coordination complexes will further isomerize to the more stable insertion products $FNMF_2$ upon blue LED (λ = 470 nm) light irradiation.

Department of Chemistry and Biochemistry, Freie Universität Berlin, Fabeckstr. 34/36, 14195 Berlin, Germany. E-mail: ghdeng@zedat.fu-berlin.de; s.riedel@fu-berlin.de

† Electronic supplementary information (ESI) available. See DOI: https://doi.org/10.1039/d3sc02313c

Results and discussion

The title complexes were produced by the reactions of laser-ablated palladium, platinum atoms and nitrogen trifluoride in solid argon, and were recorded by FTIR absorption spectroscopy with isotopic substitutions. The IR spectra in the 1150–550 cm^{-1} region using a 0.5% NF_3/Ar mixture are represented in Fig. 1 and 2. After 60 min of sample deposition, common absorption bands due to NF and NF_2 radicals are observed,[20] which decrease on annealing but slightly increase on blue LED ($\lambda = 470$ nm) light irradiation. No obvious absorption bands of molecular metal fluorides are observed. Besides these common product absorption bands, new metal dependent absorption bands were also detected, which can be classified into two groups based on their identical annealing and photochemical behaviours (labeled **A** and **B** in Fig. 1 and **C** and **D** in Fig. 2). Since some absorption bands are partially overlapped by the nitrogen trifluoride absorption bands, a difference IR spectrum taken from the spectrum after blue LED ($\lambda = 470$ nm) light irradiation minus the spectrum after 20 K annealing is obtained and represented in Fig. S1 and S2.† Similar experiments were also performed using an isotopically labelled compound $^{15}NF_3$ and a $^{14}NF_3$ + $^{15}NF_3$ mixture. The IR spectra in the selected region are shown in Fig. S1 and S2.† All observed band positions are listed in Table 1.

Experiments were also carried out with laser-ablated palladium, platinum atoms and NF_3 in excess neon. The spectra with 0.1% NF_3 and isotopic substitutions in neon are shown in Fig. S3–S6.† The same products as detected in argon are presented, but the $Pd(NF_3)$ product absorption bands are weaker than those detected in solid argon. The product absorption bands in solid neon are given in Table 1. The band positions are blue-shifted to higher wave numbers compared to those of the argon matrix.

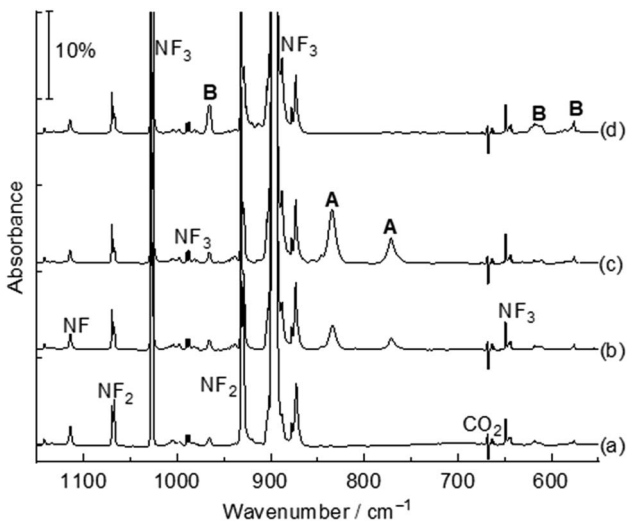

Fig. 1 Infrared spectra in the 1150–550 cm^{-1} region from co-deposition of laser-ablated Pd atoms with 0.5% NF_3 in argon. (a) After 60 min of sample deposition, (b) after annealing to 15 K, (c) after annealing to 20 K, and (d) after 10 min of blue LED ($\lambda = 470$ nm) light irradiation. **A**: $Pd(NF_3)$; **B**: $FNPdF_2$.

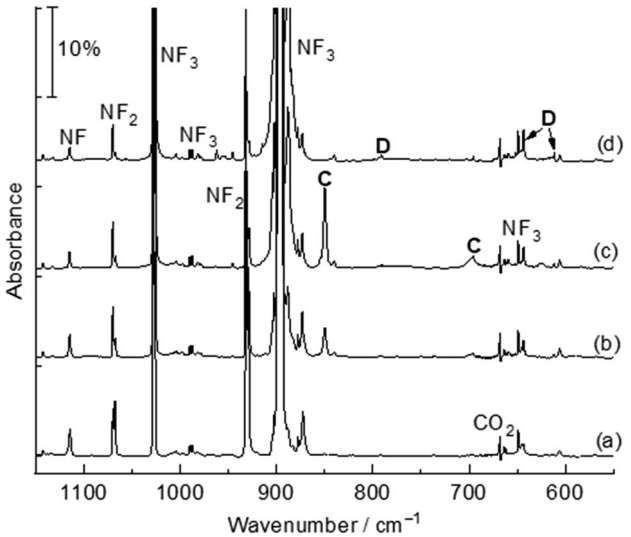

Fig. 2 Infrared spectra in the 1150–550 cm^{-1} region from co-deposition of laser-ablated Pt atoms with 0.5% NF_3 in argon. (a) After 60 min of sample deposition, (b) after annealing to 15 K, (c) after annealing to 20 K, and (d) after 10 min of blue LED ($\lambda = 470$ nm) light irradiation. **C**: $Pt(NF_3)$; **D**: $FNPtF_2$.

The absorption bands at 834.4 and 771.3 cm^{-1} labeled **A** (Fig. 1, trace c) are assigned to the Nitrogen-coordination $Pd(NF_3)$ complex. These absorption bands appeared after sample annealing to 15 K and increase remarkably when the matrix samples are annealed to 20 K, but disappeared totally under 10 min blue LED ($\lambda = 470$ nm) light irradiation. Both bands are red-shifted compared to the N–F stretching vibration (1028.1 and 898.1 cm^{-1}) modes of free NF_3 in argon.[15] In the experiment using the isotopic-labeled $^{15}NF_3$ sample, the absorption bands shift to 813.8 and 753.7 cm^{-1} with a $^{14/15}N$ isotopic shift of 20.6 and 17.6 cm^{-1} respectively. The band position and isotopic splitting in the mixed $^{14}NF_3$ + $^{15}NF_3$ (1 : 1) experiment (Fig. S1†) confirm that only one NF_3 ligand is involved. Accordingly, the two absorption bands 834.4 and 771.3 cm^{-1} are assigned to the symmetric and antisymmetric N–F stretching modes. The $Pd(NF_3)$ complex in solid neon is observed at 838.6 and 778.1 cm^{-1}, which are only 4.2 and 6.8 cm^{-1} blue-shifted from those in argon, indicating a weak matrix effect. This type of 1 : 1 metal–ligand complex with a metal coordinated by a nitrogen atom of the ligand is common for molecular complexes.[21]

In addition to the $Pd(NF_3)$ absorption bands, another group of absorption bands at 965.6, 612.3 and 575.5 cm^{-1} labeled **B** (Fig. 1, trace d) are produced after sample co-deposition. These absorption bands increased under blue LED ($\lambda = 470$ nm) light irradiation at the expense of group A absorption bands, indicating that product **B** is a structural isomer of product **A**, and is assigned to the $FNPdF_2$ complex. The 965.6 cm^{-1} absorption band is mainly a F–N stretching vibration with a large $^{14/15}N$ shift (19.9 cm^{-1}). The $^{14/15}N$ shift is close to those of 21.4 cm^{-1} in $FNCoF_2$ and 18.9 cm^{-1} in $FNRhF_2$.[16] This band position is red-shift by 153.8 cm^{-1} compared to the free NF radical (1119.4 cm^{-1}),[12] indicating a strong interaction between

Table 1 Experimentally observed vibrational frequencies (cm^{-1}) and isotopic frequency shifts (cm^{-1}) (in parentheses) of the $M(NF_3)$ and $FNMF_2$ (M = Pd, Pt) complexes in solid matrices (neon and argon) in comparison with quantum-chemical calculations. Calculated IR intensities (km mol^{-1}) are provided in square brackets (absorption bands above 400 cm^{-1} are listed)

	Obs.		Calc.		
Complexes	Ne	Ar	B3LYP[b]	CCSD (T)[b]	Assignments[c]
$Pd(NF_3)$ (**A**)	838.6 (20.5)	834.4 (20.6)	849 (22.1) [731]	878 (21.3)	sym. N–F str.
	778.1 (17.5)	771.3 (17.6)	703 (17.8) [159] × 2	813 (18.7)	asym. N–F str.
	—[a]	—[a]	610 (0.9) [11]	629 (1.5)	
	—[a]	—[a]	445 (0.1) [10] × 2	475 (0.5)	
$Pt(NF_3)$ (**C**)	869.3 (24.7)	849.5 (24.1)	901 (26.3) [811]	854 (23.4)	sym. N–F str.
	703.9 (17.5)	696.3 (17.7)	667 (17.9) [121] × 2	750 (18.5)	asym. N–F str.
	—[a]	—[a]	624 (0.3) [42]	634 (0.1)	
	—[a]	—[a]	452 (0.1) [23] × 2	476 (0.5)	
$FNPdF_2$ (**B**)	968.0 (19.2)	965.6 (19.9)	994 (22.9) [232]	—	N–F str.
	—[a]	—[a]	820 (20.7) [60]	—	N–Pd str.
	625.5 (0)	612.3 (0)	610 (<0.1) [104]	—	asym. F–Pd–F str.
	588.0 (0.3)	575.7 (0.4)	579 (0.2) (94)	—	sym. F–Pd–F str.
$FNPtF_2$ (**D**)	890.4 (20.7)	883.6 (21.2)	925 (26.6) [160]	933 (20.2)	N–F str.
	798.7 (20.2)	790.8 (20.2)	833 (18.0) [119]	804 (23.0)	N–Pt str.
	653.6 (0.3)	643.4 (0)	640 (<0.1) [109]	608 (<0.1)	asym. F–Pt–F str.
	622.6 (0)	611.5 (0.2)	608 (<0.1) [79]	578 (<0.1)	sym. F–Pt–F str.

[a] Absorption bands not observed or too weak. [b] Harmonic frequencies calculated at the B3LYP/aug-cc-pVTZ(-PP) and CCSD(T)/aug-cc-pVTZ(-PP) levels are listed for the ^{106}Pd and ^{195}Pt isotopologues. The complete set of vibrational frequencies is provided in ESI Tables S1 and S2. For the CCSD(T) calculations no intensities are available. [c] Tentative assignments based on calculated vibrational displacement vectors.

nitrogen and palladium. Two low bands are attributed to the PdF_2 antisymmetric and symmetric stretching modes, which are lower than 652.1 and 586.1 cm^{-1} in $OPdF_2$.[22] The palladium isotope pattern of these bands is not resolved, and only the band at 575.5 cm^{-1} displays a small 0.4 cm^{-1} shift with the $^{15}NF_3$ sample. The Pd–N stretch is too weak to be observed. The $FNPdF_2$ complex in solid neon is observed at 968.0, 625.5 and 588.0 cm^{-1}. The band positions are 2.4, 13.2 and 2.3 cm^{-1} blue-shifted from argon to neon. The observation of **B** directly after sample deposition indicates that it can be generated during the sample deposition process initiated by the excitation from the ablation plume.

Similar absorption bands are also observed in the platinum experiments. The product absorption bands at 849.5 and 696.3 cm^{-1} labeled **C** (Fig. 2, trace c) are assigned to the $Pt(NF_3)$ complex. These bands shifted to 825.4 and 678.6 cm^{-1} with $^{15}NF_3$, and only the pure isotopic counterparts were observed in the 1 : 1 mixed $^{14}NF_3$ + $^{15}NF_3$ experiment. The band positions and isotopic frequency shifts (24.1 and 17.7 cm^{-1}) are close to those of the $Pd(NF_3)$ complex, indicating similar bonding mode between palladium and platinum. The bands at 883.6, 790.8, 643.4 and 611.5 cm^{-1} labeled **D** (Fig. 2, trace d) that appeared upon co-deposition and increased after blue LED (λ = 470 nm) light irradiation are assigned to the $FNPtF_2$ molecule. The $^{15}NF_3$ counterparts are detected at 862.4, 770.6, 643.4 and 611.3 cm^{-1} with isotopic shifts of 21.2, 20.2, 0 and 0.2 cm^{-1}. These absorption bands belong to the F–N and Pt–N stretching vibration as well as PtF_2 antisymmetric and symmetric stretching modes. The $Pt(NF_3)$ and $FNPtF_2$ complexes are detected at 849.5, 696.3 and 890.4, 798.7, 653.6, and 622.6 cm^{-1} respectively in solid neon. The photoisomerization reaction of metal nitrogen trifluoride complexes (**A** and **C**) to $FNMF_2$ (**B** and **D**) is reproducible in the neon matrix. No similar product absorption bands are observed in the Ni + NF_3 experiments.

The structures and vibrational frequencies of $M(NF_3)$ and $FNMF_2$ (M = Pd, Pt) in the closed shell singlet ground state were calculated at the B3LYP/aug-cc-pVTZ(-PP) and CCSD(T)/aug-cc-pVTZ(-PP) levels (for details see the ESI†). Among the four isomers, the $FNMF_2$ isomer has the lowest energy (Fig. S7†). As shown in Fig. 3, the $Pd(NF_3)$ and $Pt(NF_3)$ complexes possess an $^1A_1$ electronic ground state and nitrogen trifluoride is coordinated to the metal center through nitrogen forming a C_{3v} structure. The triplet states of $[Pd(NF_3)]$ and $[Pt(NF_3)]$ are less stable by 33.0 and 25.1 kcal mol^{-1} at the CCSD(T)/aug-cc-pVTZ(-PP)//B3LYP/aug-cc-pVTZ(-PP) level. The N–F bond distance in the nitrogen trifluoride ligand is significantly longer (1.399 Å for Pd and 1.409 Å for Pt) than in free nitrogen trifluoride (1.371 Å).[23] The calculated Pd–N distance in the complex is slightly longer (2.073 Å) than that of PdNCCN (1.948 Å)[24] and PdNNO

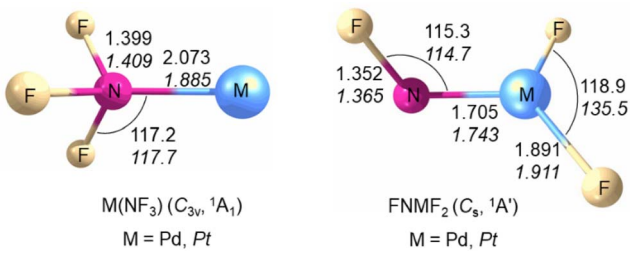

Fig. 3 Calculated structures (bond lengths in Ångstroms and bond angles in degrees) of $M(NF_3)$ (M = Pd, Pt) and $FNPtF_2$ at the CCSD(T)/aug-cc-pVTZ(-PP) level and of $FNPdF_2$ at the B3LYP/aug-cc-pVTZ(-PP) level of theory.

(2.003 Å).[25] The predicted Pt–N bond distance is 1.885 Å and close to that of 1.893 Å in the PtNNO complex.[25] The $FNPdF_2$ and $FNPtF_2$ molecules are predicted to have an $^1A'$ ground state with a C_s symmetric structure, and are more stable than the $Pd(NF_3)$ and $Pt(NF_3)$ isomers by 41.6 and 80.9 kcal mol^{-1}, respectively. The triplet $FNPdF_2$ and $FNPtF_2$ species are 9.8 and 16.6 kcal mol^{-1} higher in energy than the corresponding molecules in the singlet state. The computed Pd–N distance of 1.705 Å in $FNPdF_2$ is significantly shorter with respect to the $Pd–N^{Dip}$ bond length of 1.872(3) Å in the (CAAC)Pd(Dip) compound [CAAC = cyclic (alkyl)(amino)carbene, Dip = 2,6-diisopropylphenyl][26] and in the range of those for calculated palladium nitrenes (1.8–2.0 Å).[27] The predicted Pt–N bond length of 1.743 Å and shorter than that of the linear two-coordinated platinum complex $Pt(NC^tBu_2)_2$ [1.814(4) Å, 1.818(4) Å],[28] but longer than that of the binary molecule PtN (1.703 Å).[29] The short bond length and large $^{14/15}N$ isotopic shift indicate that the M–N bond in $FNMF_2$ is a double bond with a nitrene structure in which the metal shows a formal oxidation state +II, which are similar to the Rh–N bond in the $FNRhF_2$ molecule.[16] The calculated structures of the F_2NMF and NMF_3 (M = Pd, Pt) isomers are shown in Fig. S8.†

The assignment of the $M(NF_3)$ and $FNMF_2$ (M = Pd, Pt) complexes is supported by theoretical calculations at the B3LYP and CCSD(T) levels of theory. As listed in Table 1, similar to the $FNRhF_2$ complex,[16] the calculated absorption band positions and observed experimental values of the F–N and N–M stretching frequencies in the $FNMF_2$ complexes do not match perfectly due to strong vibrational coupling between these two vibrational modes. Additionally, the predicted wavenumbers as well as isotopic shifts in other vibrational stretching modes in the complexes $M(NF_3)$ and $FNMF_2$ (M = Pd, Pt) show good agreement with the experimental values. All in all, the comparison between the computed and observed IR spectra strongly supports that the experimentally observed products are the nitrogen trifluoride complex $M(NF_3)$ and $FNMF_2$ (M = Pd, Pt) molecules. The calculated vibrational frequencies and intensities of the possible further isomers F_2NMF and NMF_3 are shown in Tables S1 and S2.† However, both hypothetical isomers show different spectral signatures than our observed spectra, which further supports our assignment of the experimental bands. The relative energies (kcal mol^{-1}) of different isomers of F_3NM (M = Pd, Pt) are given in Table S3.†

The bonding of $Pd(NF_3)$ and $Pt(NF_3)$ complexes is of particular interest. By taking $Pt(NF_3)$ as an example. Fig. 4 shows the highest-lying occupied molecular orbitals. The HOMO and HOMO−1 are metal based 6s and $5d_{xy/x^2-y^2}$ nonbonding orbitals. The HOMO−2 is doubly degenerate metal d_π orbital and composed of metal $5d_{xz/yz}$ and the LUMO of nitrogen trifluoride. The HOMO−3 and HOMO−4 are only composed of ligand orbitals. The HOMO−5 is a ligand-based orbital that comprises some weak ligand to metal σ donation. Previous reports have proved that the bonding of lone-pair ligands to transition metals is generally consisted of σ donation from the ligand to the metal and π back-donation from the metal to the ligand.[2] Based on this assumption, the Pt $5d_{z^2}$ orbital should be considered as an empty σ orbital to accept electron donation of

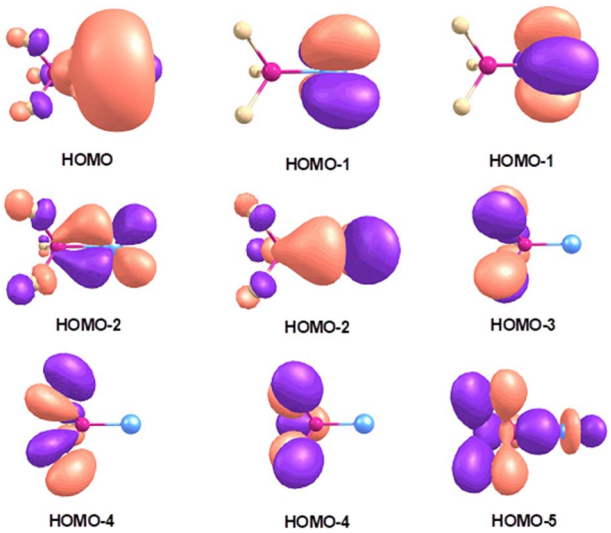

Fig. 4 Shape of the selected highest-lying occupied molecular orbitals of $Pt(NF_3)$ at the B3LYP/aug-cc-pVTZ level.

the NF_3 HOMO and the back-donation of the Pt π electrons to the NF_3 LUMO upon the formation of the $Pt(NF_3)$ complex. The donation interaction between the HOMO of NF_3 and a vacant Pt $5d_{z^2}$ orbital with σ symmetry stabilizes the Pt–N and N–F bonds, while the back-donation from the Pt d_π orbital to the NF_3 LUMO causes the destabilization of the N–F bond. Consistent with this notion, the N–F stretching frequencies of the $Pt(NF_3)$ complex are red-shifted compared to the neutral nitrogen trifluoride. The $Pd(NF_3)$ complex has a quite similar bonding situation to $Pt(NF_3)$. The palladium complex shows a lower N–F stretching frequency and the comparison with the platinum species suggests that the palladium complex has an even stronger back-donation. This shift can be explained by the different energy levels of the valence $(n-1)$d and ns orbitals of the 4d and 5d transition metal atoms, which has been discussed for group 10 transition metal nitrous oxide complexes[25] as well as group 11 transition metal carbonyl complexes.[30]

The spectra illustrated in Fig. 1 and 2 clearly suggest that the N-coordination $M(NF_3)$ complexes are generated by the reactions of ground state palladium (^1S) and platinum (^3D) atoms with nitrogen trifluoride in solid neon and argon matrices. These association reactions are calculated to be exothermic by 11.0 (Pd), and 28.5 kcal mol^{-1} (Pt) [CCSD(T)/aug-cc-pVTZ level], respectively, and require negligible activation energy, as the $M(NF_3)$ absorption bands increase on annealing, while a similar reaction product for nickel is predicted to be endothermic and was not observed. The bonding energies of nitrogen trifluoride are very close to those of the PdNNO and PtNNO complexes,[25] which are produced between Pd/Pt metals and nitrous oxide, but lower than that of PdNCCN and PtNCCN cyanogen complexes.[24] The $M(NF_3)$ complexes rearrange to the $FNMF_2$ isomers under blue LED (λ = 470 nm) light irradiation. These isomerization reactions are computed to be exothermic by 41.6 (Pd) and 80.9 (Pt) kcal mol^{-1} at the CCSD(T)/aug-cc-pVTZ(-PP)//B3LYP/aug-cc-pVTZ(-PP) level of theory. The isomeric pathway is predicted to proceed *via* two transition states involving the sequence $M(NF_3)$

→ F_2NMF → $FNMF_2$. Fig. S9† shows the pathway where the first step $M(NF_3)$ → F_2NMF involves an activation energy barrier of 24.6 (Pd) and 19.1 (Pt) kcal mol^{-1}. The second step F_2NMF → $FNMF_2$ requires to cross a lower barrier of 10.0 (Pd) and 17.6 (Pt) kcal mol^{-1}. Both two energy barriers 34.6 (Pd) and 36.7 (Pt) kcal mol^{-1} are lower than the energy of LED ($\lambda = 470$ nm) light (60.8 kcal mol^{-1}). Consistent with the low bonding energy, the $M(NF_3)$ complexes underwent decomposition to form metal atoms and NF_3 molecules when the matrix samples were subjected to blue LED ($\lambda = 470$ nm) light photolysis and result in low efficiency to yield $FNMF_2$ complexes. Further work is currently underway to study the reactions of group 10 metal atoms with phosphorus trifluoride (PF_3).

Conclusions

In summary, we described the formation of N-coordination nitrogen trifluoride complexes $M(NF_3)$ (M = Pd, Pt) by the reaction of laser-ablated group 10 transition metal atoms with NF_3 in solid neon and argon matrices. These molecular complexes were characterized by matrix-isolation infrared absorption spectroscopy and quantum-chemical calculations. The complexes rearrange to the $FNMF_2$ isomer under blue LED ($\lambda = 470$ nm) light irradiation, which is identified to be a fluoronitrenoid complex with a N–M double bond. The bonding in these nitrogen trifluoride complexes involves the electron donation of the HOMO of the nitrogen trifluoride to the empty metal d_{z^2} orbital and back-donation of the metal π electrons to the LUMO of nitrogen trifluoride. Although the detected metal nitrogen trifluoride products have low thermodynamic stability and can only be isolated in cryogenic matrices, they enrich and extend the arsenal of transition metal coordination chemistry and provide a deeper understanding of the fluorine specific interactions.

Data availability

Data supporting this manuscript is available within the ESI† and available on request.

Author contributions

GD planned and performed the experiments and carried out the quantum chemical calculations. He wrote the first draft of the manuscript. YL performed some of the experiments. TS helped with the design of the experiments and proof read the manuscript. SR guided and advised the project and proof read the manuscript.

Conflicts of interest

There are no conflicts to declare.

Acknowledgements

We gratefully acknowledge the Zentraleinrichtung für Datenverarbeitung (ZEDAT) of the Freie Universität Berlin for the allocation of computing resources. We thank the ERC Project HighPotOx as well as the CRC 1349 (SFB 1349) Fluorine Specific Interactions – Project-ID 387284271 – for continuous support. Open access funding was enabled and organized by Projekt DEAL. G. D thanks the Alexander von Humboldt Foundation (AvH) for a research scholarship.

Notes and references

1 (*a*) L. Rocchigiani and M. Bochmann, *Chem. Rev.*, 2021, **121**, 8364; (*b*) J. Mas-Roselló, C. J. Cope, E. Tan, B. Pinson, A. Robinson, T. Smejkal and N. Cramer, *Angew. Chem., Int. Ed.*, 2021, **60**, 15524; (*c*) C. V. Wilson, D. Kim, A. Sharma, R. X. Hooper, R. Poli, B. M. Hoffman and P. L. Holland, *J. Am. Chem. Soc.*, 2022, **144**, 10361.
2 G. Frenking and N. Fröhlich, *Chem. Rev.*, 2000, **100**, 717.
3 M. F. Zhou and G. Frenking, *Acc. Chem. Res.*, 2021, **54**, 3071.
4 O. Ruff, J. Fischer and F. Luft, *Z. Anorg. Allg. Chem.*, 1928, **172**, 417.
5 (*a*) P. Antoniotti, L. Operti, R. Rabezzana, F. Turco and G. A. Vaglio, *Int. J. Mass Spectrom.*, 2006, **255–256**, 225; (*b*) P. Antoniotti, P. Benzi, S. Borocci, C. Demaria, M. Giordani, F. Grandinetti, L. Operti and R. Rabezzana, *Chem. - Eur. J.*, 2015, **21**, 15826; (*c*) P. Antoniotti, P. Benzi, D. Marabello and D. Rosso, *ACS Omega*, 2020, **5**, 4907.
6 R. K. Belter, *J. Fluorine Chem.*, 2015, **175**, 110.
7 E. P. L. Hunter and S. G. Lias, *J. Phys. Chem. Ref. Data*, 1998, **27**, 413.
8 (*a*) O. de La Luz Rojas, *J. Am. Chem. Soc.*, 1977, **99**, 2902; (*b*) K. R. S. Chandrakumar and S. Pal, *J. Phys. Chem. A*, 2002, **106**, 11775; (*c*) P. Antoniotti, S. Borocci and F. Grandinetti, *Eur. J. Inorg. Chem.*, 2004, **2004**, 1125.
9 A. Boutalib, *J. Phys. Chem. A*, 2003, **107**, 2106.
10 Q. Luo, Q. S. Li, Y. M. Xie, R. B. King and H. F. Schaefer, *J. Chem. Theory Comput.*, 2011, **7**, 131.
11 T. Leyssens, D. Peeters, A. G. Orpen and J. N. Harvey, *Organometallics*, 2007, **26**, 2637.
12 K. M. Pei, J. Liang and H. Y. Li, *J. Mol. Struct.*, 2004, **690**, 159.
13 X. F. Wang, L. Andrews, R. Lindh, V. Veryazov and B. O. Roos, *J. Phys. Chem. A*, 2008, **112**, 8030.
14 (*a*) L. Andrews, X. F. Wang, R. Lindh, B. O. Roos and C. J. Marsden, *Angew. Chem., Int. Ed.*, 2008, **47**, 5366; (*b*) L. Andrews, X. F. Wang and B. O. Roos, *Inorg. Chem.*, 2009, **48**, 6594; (*c*) X. F. Wang and L. Andrews, *Dalton Trans.*, 2009, 9260; (*d*) X. F. Wang, J. T. Lyon and L. Andrews, *Inorg. Chem.*, 2009, **48**, 6297; (*e*) T. Stüker, X. X. Xia, H. Beckers and S. Riedel, *Chem. - Eur. J.*, 2021, **27**, 11693.
15 Y. Gong and L. Andrews, *Inorg. Chem.*, 2012, **51**, 667.
16 T. Stüker, T. Hohmann, H. Beckers and S. Riedel, *Angew. Chem., Int. Ed.*, 2020, **59**, 23174.
17 (*a*) M. H. Chen, H. Lu, J. Dong, L. Miao and M. Zhou, *J. Phys. Chem. A*, 2002, **106**, 11456; (*b*) M. F. Zhou, M. H. Chen, L. N. Zhang and H. Lu, *J. Phys. Chem. A*, 2002, **106**, 9017; (*c*) X. F. Wang, L. Andrews and C. J. Marsden, *Chem. - Eur. J.*, 2008, **14**, 9192; (*d*) X. F. Wang and L. Andrews, *Organometallics*, 2008, **27**, 4885; (*e*) X. Liu, X. F. Wang, B. Xu and L. Andrews, *Chem. Phys. Lett.*, 2012, **523**, 6; (*f*)

Z. Pu, F. Li, J. W. Qin, B. Y. Ao, P. Shi and M. B. Shuai, *J. Phys. Chem. A*, 2018, **122**, 3541.

18 (*a*) J. Berkowitz, J. P. Greene, J. Foropoulos and O. M. Nesković, *J. Chem. Phys.*, 1984, **81**, 6166; (*b*) S. T. Gibson, J. P. Greene and J. Berkowitz, *J. Chem. Phys.*, 1985, **83**, 4319.

19 F. Blanco, I. Alkorta, I. Rozas, M. Solimannejad and J. Elguero, *Phys. Chem. Chem. Phys.*, 2011, **13**, 674.

20 M. E. Jacox and D. E. Milligan, *J. Chem. Phys.*, 1967, **46**, 184.

21 (*a*) W. B. Tolman, *Angew. Chem., Int. Ed.*, 2010, **49**, 1018; (*b*) H.-J. Himmel and M. Reiher, *Angew. Chem., Int. Ed.*, 2006, **45**, 6264; (*c*) L. Andrews and A. Citra, *Chem. Rev.*, 2002, **102**, 885.

22 L. Li, H. Beckers, T. Stüker, T. Lindič, T. Schlöder, D. Andrae and S. Riedel, *Inorg. Chem. Front.*, 2021, **8**, 1215.

23 J. Sheridan and W. Gordy, *Phys. Rev.*, 1950, **79**, 513.

24 X. T. Chen, Z. X. Xiong, L. Andrews and Y. Gong, *Inorg. Chem.*, 2020, **59**, 6489.

25 X. Jin, G. Wang and M. F. Zhou, *J. Phys. Chem. A*, 2006, **110**, 8017.

26 A. Grünwald, B. Goswami, K. Breitwieser, B. Morgenstern, M. Gimferrer, F. W. Heinemann, D. M. Momper, C. W. M. Kay and D. Munz, *J. Am. Chem. Soc.*, 2022, **144**, 8897.

27 A. Grünwald and D. Munz, *J. Organomet. Chem.*, 2018, **864**, 26.

28 A. W. Cook, P. Hrobárik, P. L. Damon, D. Najera, B. Horváth, G. Wu and T. W. Hayton, *Inorg. Chem.*, 2019, **58**, 15927.

29 A. Citra, X. F. Wang, W. D. Bare and L. Andrews, *J. Phys. Chem. A*, 2001, **105**, 7799.

30 P. H. Kasai and P. M. Jones, *J. Phys. Chem.*, 1985, **89**, 1147.